

Fermi surfaces and electronic topological transitions in metallic random alloys.

I. The influence on equilibrium properties

E. Bruno, B. Ginatempo, and E. S. Giuliano

Dipartimento di Fisica, Università di Messina, Salita Sperone 31, 98166 Messina, Italy

(Received 13 February 1995)

In this paper we address the question of how the so-called electronic topological transitions (ETT's) can affect the physical properties of metallic random alloys, extending the existing theory in order to include substitutional disorder. The ETT's, or, as sometimes called, the Lifshitz $2\frac{1}{2}$ transitions, occur when the chemical potential passes through a Van Hove singularity on changing the thermodynamic state of a metal. That can be easily achieved by alloying. As a consequence, the Fermi-surface topology changes and a number of transport as well as equilibrium properties show anomalies, when studied versus the concentration. We show that these anomalies might be only slightly affected by disorder scattering and/or finite temperatures. Our theoretical results, which hold in a neighborhood of the ETT, predict anomalies in correspondence to such variations of Fermi-surface connectivity for the equilibrium volumes and total energies. In particular, our theory predicts deviations of the alloy lattice parameter from Vegard's rule. These are confirmed by our *ab initio* Korringa-Kohn-Rostoker-coherent-potential-approximation calculations for the $\text{Ag}_c\text{Pd}_{1-c}$ system. For this system the largest deviation from Vegard's rule occurs as the *d*-conduction bands are completely filled. Detailed calculations of the $\text{Ag}_c\text{Pd}_{1-c}$ Fermi surfaces are presented in a separate paper (II).

I. INTRODUCTION

Since the seminal work of Lifshitz,¹ a large amount of theoretical and experimental work was devoted to the study of electronic topological transitions (ETT's) in metals. Recently, some reviews of these topics²⁻⁴ were published and we need not give here an extended list of references to previous work. The purpose of the present paper and of its companion,⁵ quoted in the following as II, is to discuss the extension of the ETT theory to the interesting case of random metallic alloys. We shall obtain some results for this class of systems. Namely, we shall find a formula, exact in a proximity of an ETT, for the electronic part of the grand potential at finite temperatures and in the presence of substitutional disorder. Moreover, we shall discuss the influence of ETT's on the variation of the alloy equilibrium volume versus the electron per atom ratio (e/a). These effects might be responsible for deviations from Vegard's law. In Paper II we shall present an accurate, total-energy calculation for the very interesting $\text{Ag}_c\text{Pd}_{1-c}$ system, which, as we shall see, undergoes five distinct ETT's.

The ETT theory moves in the framework of Landau's Fermi-liquid theory.⁶ In that context, the peculiar features of the metallic state and the relevant part of the quasiparticle spectrum are deeply related to the geometrical properties of the Fermi surface (FS).^{7,8} Thus, for instance, the differential geometry of the FS manifold determines the quasiparticle velocities and mass tensor. Therefore, changes in the FS topology, as argued by Lifshitz, cause relevant effects on many physical properties of metals.

We have an ETT, or Lifshitz $2\frac{1}{2}$ "phase transition" when, on varying some thermodynamical variable, the

chemical potential crosses a stationary point of the band structure. Under this circumstance the FS changes its connectivity. Namely, one may have the formation or closure of electron or hole pockets, the opening or the disruption of necks. Accordingly, the density of states (DOS) includes a special term proportional to a step function: the Van Hove singularity.⁹

As shown by Lifshitz,¹ the electronic contribution to the grand potential also includes a special term. This implies that many physical properties, such as specific heat, resistivity, sound absorption, and electron-phonon coupling will be affected.²⁻⁴ In particular, the most spectacular effect occurs for the diffusion thermopower which, at $T=0$ and in the absence of disorder, diverges with exponent $\frac{1}{2}$. This notwithstanding, as Varlamov, Egorov, and Pantsulaya² discuss, an ETT is not a phase transition, since divergences are expected *only* at $T=0$. Any finite temperature as well as any disorder scattering, in fact, will turn the divergences into finite peaks. These, often, remain observable even at fairly large temperature or, in random alloys, well beyond the impurity limit.

The experimental investigation of ETT's can be performed either at fixed e/a , by applying to the sample pressures or uniaxial stresses² (usually large) or by varying the e/a ratio by alloying. The existing theory, reviewed by Varlamov, Egorov, and Pantsulaya² and Blanter *et al.*,³ describes accurately the first class of experiments. However, in practice, the study of ETT's versus e/a in alloys often requires a much simpler experimental apparatus. Thus, a theory able to deal with the substitutional disorder is desirable. We have to quote here the effort of Blanter *et al.*,³ which studied in the presence of finite lifetimes, several observables in an ETT proximity, in various asymptotic regimes. We wish to

contribute, with the present paper, to this field with an explicit and straightforward formula concerning the special part of the grand potential in the presence of disorder scattering.

The rest of this paper is organized as follows. In Sec. II we extend the ETT theory including both finite temperature and disorder scattering effects and address the study of the equilibrium unit-cell volume versus the concentration. To be more explicit, in Sec. II A, assuming infinite lifetimes and zero temperature, we shall derive in the framework of Lifshitz's theory a formula for the variation of the alloy lattice parameter with the ETT "order parameter" or with the e/a ratio. These results shall be extended including finite quasiparticle lifetimes at $T=0$ in Sec. II B. The major point there shall be the introduction of a complex order parameter, which allows us to develop an analytic theory. In this, the special part of the grand potential is not longer singular, because the singularities are smoothed by disorder. We shall take advantage of the above analytic features in Sec. II C, where the theory will be extended, in full generality, to finite temperatures. This shall be accomplished through the introduction of a complex dimensionless temperature that enters in the thermal broadening of thermodynamic potentials. These broadening effects, which shall be studied in more detail in several asymptotic regimes, however, may not cancel completely the anomalies predicted by Lifshitz's theory. In Sec. III these findings, namely, the expected anomalies of the lattice parameter, are illustrated by means of our *ab initio* Korringa-Kohn-Rostoker-coherent-potential-approximation (KKR-CPA) calculations for the $\text{Ag}_c\text{Pd}_{1-c}$ alloys. These calculations, which shall be discussed in Paper II show that anomalies in the above quantities actually occur at concentrations at which the FS topology changes. These behaviors shall be compared with measurements of the equilibrium lattice parameter¹⁰ and the diffusion thermoelectric power.¹¹ In Sec. IV we shall draw our conclusions and make final remarks.

II. THE INFLUENCE OF ETT'S ON SOME THERMODYNAMIC PROPERTIES OF RANDOM BINARY ALLOYS

A. Pure systems at $T=0$

In this section we shall briefly recall some previous results^{2,3} of the theory of ETT's in order to extend them to the case of random binary metallic alloys.

The thermodynamic extensive variable related to the atomic concentrations of each alloy component is, in the present case, the total number of electrons, N , which, at $T=0$, is given by

$$N = \int_{-\infty}^{\mu} dE n(E) = \int_{-\infty}^{\mu} dE [cn_A(E) + (1-c)n_B(E)]. \quad (1)$$

In Eq. (1), $n_A(E)$ and $n_B(E)$ are the A and B projected DOS, c and $1-c$ the atomic concentrations of the A and B species, and μ the electronic chemical potential. In the following discussion we shall use, as independent thermo-

dynamic variables, either N or μ and, accordingly, the appropriate thermodynamic potential shall be the free energy, $F(T, V, N)$, or the grand potential, $\Omega(T, V, \mu)$.

Let us consider the case of an electronic crystal band having a minimum, a maximum, or a saddle point at some energy $E = \epsilon_c$. Under these circumstances, a change in the connectivity of the Fermi surface, or ETT, occurs when, on varying some thermodynamical variable, the chemical potential μ passes through ϵ_c . In the case of a minimum (maximum), this corresponds to the appearance (disappearance) in the FS of voids of electrons. On the other hand, in the case of a saddle point at ϵ_c , necks open (or close) in the Fermi surface as the chemical potential is increased. In all the above circumstances, following Lifshitz,¹ we shall consider the DOS as the sum of a "regular" contribution, $n_0(E)$, due to bands not involved in the ETT, and a "special" term, $n_1(E)$, due to the band with an extremum at $E = \epsilon_c$, i.e.,

$$n(E) = n_0(E) + n_1(E). \quad (2)$$

In the present paper, the energy dependence of the regular term in Eq. (2) shall be supposed smooth. More relevant, for our purposes, shall be the behavior of the special term. Interestingly, analytic expressions for $n_1(E)$ can be obtained, for energies close enough to ϵ_c . In fact, in a proximity of the ETT, the dispersion relation for the relevant band may be approximated by simple analytic forms. Namely, in the cases of maxima or minima in the band structure, equienergy surfaces in the momentum space are well approximated by ellipsoids. Thus, the relevant part of the spectrum may be represented as follows:

$$\epsilon_1(\mathbf{p}) = \epsilon_c \pm \frac{1}{2} \left[\frac{p_x^2}{m_x} + \frac{p_y^2}{m_y} + \frac{p_z^2}{m_z} \right] - i\eta(\mathbf{p}), \quad (3a)$$

where m_i are the principal values of the mass tensor, and, where the upper or lower sign holds in the case of a minimum or a maximum.

In Eq. (3a) we have introduced an imaginary part, $\eta(\mathbf{p})$, in the spectrum. This is designed in order to incorporate the effects of substitutional disorder and, thus, vanishes in the case of a perfect crystal, whereas, if impurity scattering is present, it turns out to be inversely proportional to the electron lifetimes, $\eta(\mathbf{p}) \sim \hbar/\tau(\mathbf{p})$. In a similar way, when studying the neighborhood of a saddle point, we shall use a simple analytic approximation for the relevant part of the spectrum. Namely, we write

$$\epsilon_1(\mathbf{p}) = \epsilon_c \pm \frac{1}{2} \left[\frac{p_x^2}{m_x} - \frac{p_y^2}{m_y} - \frac{p_z^2}{m_z} \right] - i\eta(\mathbf{p}), \quad (3b)$$

where the upper and lower signs correspond to saddle points of different indices 1 and 2, respectively. For the sake of completeness we notice that, besides the cases described by Eqs. (3a) and (3b), some other, less common, ETT's are possible. Such is, for instance, the toroidal neck disruption,³ which is known to occur in wurzite-type crystals.¹² However, these more exotic ETT's will not be discussed in the present paper.

It is worth noting that the upper sign in Eqs. (3a) and

(3b) corresponds to the circumstance in which, on increasing the chemical potential, new voids of electrons form or necks close. In both these cases, the FS connectivity, i.e., the number of simply connected regions, increases. On the other hand, in the cases in which the lower sign applies in Eqs. (3a) and (3b), voids disappear or necks open and the connectivity decreases as μ is raised.

Once the shape of the band involved in the ETT, i.e., Eq. (3a) or (3b), is known, the special contribution to the DOS may be calculated integrating over the Brillouin zone the corresponding contribution to the spectral function,⁴

$$A_1(\mathbf{p}, E) = -\frac{1}{\pi} \text{Im} \left\{ \frac{1}{E - \varepsilon_1(\mathbf{p})} \right\} \quad (4)$$

as follows:

$$n_1(E) = (2V/h^3) \int d\mathbf{p} A_1(\mathbf{p}, E). \quad (5)$$

The effects of the inclusion of impurity scattering shall be discussed in Secs. II B and II C. In the present section we shall assume the spectrum real, that is to say, $\eta(\mathbf{p})=0$. Under these circumstances, the spectral function reduces to δ contributions,

$$A_1(\mathbf{p}, E) = \delta(E - \varepsilon_1(\mathbf{p})), \quad (4')$$

and the integral in Eq. (5) is easily carried out. The result, for a three-dimensional metal,¹ turns out to be singular,

$$n_1(E) = \alpha |z|^{1/2} \Theta(z). \quad (6)$$

Namely, the special contribution to the DOS, $n_1(E)$, is proportional to the step function, $\Theta(x)=1$ for $x > 0$ and $\Theta(x)=0$ for $x < 0$. The discontinuity in the first derivative of the DOS arising from the contribution of Eq. (6) is also known in solid state theory as a Van Hove singularity.⁹

In Eq. (6) we have introduced the quantity

$$z = \pm(E - \varepsilon_c), \quad (7)$$

where the upper or lower sign has the same meaning as in Eq. (3a) or (3b), i.e., it corresponds to an increase or a decrease of the FS connectivity. Although it is an intensive quantity and ETT are not proper phase transitions, nevertheless, as we shall see later, z plays the role of an "order parameter" in the context of Lifshitz's theory. Moreover, in Eq. (6) we have defined the quantity α as follows,

$$\alpha = \pm V |2m_1 m_2 m_3|^{1/2} / (\pi^2 \hbar^3) \quad (8)$$

where the upper (lower) sign has to be used when the band shape is described by Eqs. (3a), (3b). The conventions used in this paper for the signs in Eqs. (7) and (8) are illustrated in Fig. 1, for different types of Van Hove singularities.

Similarly to the DOS, also the thermodynamic potentials include a special contribution related to the band involved in the ETT. In particular, the grand potential,

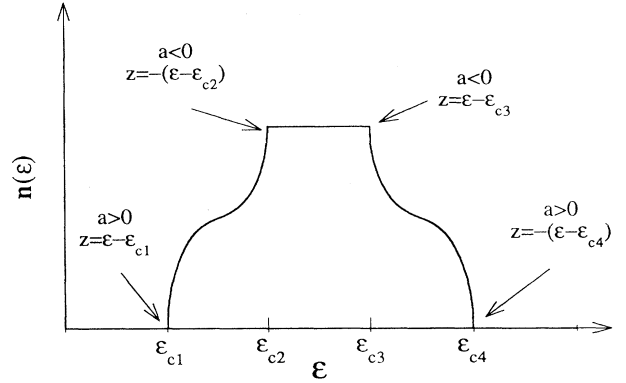


FIG. 1. A sketch of a typical one-band DOS. The Van Hove singularities corresponding to the band minimum, a saddle point of index 2, a saddle point of index 1, and the band maximum occur, respectively, at the energies ε_{c1} , ε_{c2} , ε_{c3} , and ε_{c4} . The sign conventions used in the text [see Eqs. (6) and (6')] for a and z in a proximity of each type of singularity are also shown.

$$\Omega(T, V, \mu) = - \int_{-\infty}^{\infty} dE [e^{(E-\mu)/(k_B T)} + 1]^{-1} \times \int_{-\infty}^E dE' n(E') \quad (9)$$

can be written as the sum of a regular and a special, ETT-related, term, $\Omega(T, V, \mu) = \Omega_0(T, V, \mu) + \Omega_1(T, V, \mu)$. Here we report the result for $\Omega_1(T, V, \mu)$ in the vicinity of the ETT, at $T=0$ in the absence of impurity scattering,¹

$$\Omega_1(T, V, \mu) = -\frac{4}{15} \alpha |z|^{5/2} \Theta(z) = -\frac{4}{15 \alpha^4} n_1^5(\mu). \quad (10)$$

It is worth noting that $\Omega_1(T, V, \mu)$ is always negative in the cases described by Eq. (3a), i.e., of creation of electron pockets or destruction of hole pockets, and positive when the opening or the disruption of a neck occurs.

As we shall discuss in Secs. II B and II C, the singularity in Eq. (10) is smeared out at any $T > 0$, due to the broadening of the Fermi function in Eq. (9), and, even at zero temperature, by finite-lifetime effects.^{2,3} In the present section, following Ref. 3, we shall analyze the change in the thermodynamic potentials due to an isotropic variation of the unit-cell volume and extend the discussion to the case of a binary solid solution.

In order to overcome the problems arising from the nonanalyticity of the ETT theory in the $T=0$, $\eta(\mathbf{p})=0$ limit, in the present subsection, unless otherwise stated, we shall consider only the regime of concentrations for which $z > 0$. On the other hand, for $z < 0$, in the above limit, the corrections due to the ETT are trivially zero.

Here we need to study the order parameter variation versus the total number of electrons (or the concentration). For this purpose we shall consider two different thermodynamical paths. First we use a path along which the volume is constrained to its equilibrium value, $V_{\text{eq}}(N)$. This is defined as the value that minimizes the free energy, at fixed T and N . Along the above path, z satisfies the differential equation

$$\frac{dz}{dN} = \pm(\gamma - \gamma_c) \frac{dV_{\text{eq}}(N)}{dN} \pm(\lambda - \lambda_c), \quad (11)$$

where the signs correspond to that given in Eq. (7), and where

$$\gamma = \left[\frac{\partial \mu}{\partial V} \right]_N, \quad \lambda = \left[\frac{\partial \mu}{\partial N} \right]_V, \quad (12)$$

and

$$\gamma_c = \left[\frac{\partial \epsilon_c}{\partial V} \right]_N, \quad \lambda_c = \left[\frac{\partial \epsilon_c}{\partial N} \right]_V. \quad (13)$$

The thermodynamic derivatives of the chemical potential in Eqs. (12) may be evaluated from the identities obtained deriving explicitly Eq. (1) with respect to V and N . Namely,

$$\gamma = -\frac{1}{n(\mu)} \int_{-\infty}^{\mu} dE \left[\frac{\partial n(E)}{\partial V} \right]_N \quad (14)$$

and

$$\lambda = \frac{1}{n(\mu)} \left[1 - \int_{-\infty}^{\mu} dE \left[\frac{\partial n(E)}{\partial N} \right]_V \right]. \quad (15)$$

Equations (14) and (15) link the changes in the chemical potential to the variation of the band shapes along different thermodynamic paths. The evaluation of the quantities defined in Eqs. (12) and (13) requires, of course, a detailed calculation of the electronic structure of the system.

On the other hand, if we consider a second thermodynamic path along which N is kept *constant*, we obtain a useful relationship, already derived in Ref. 3, i.e.,

$$\left[\frac{\partial z}{\partial V} \right]_N = \pm(\gamma - \gamma_c). \quad (16)$$

Let us now call $V_c(N)$ the volume at which the ETT occurs for a given N . There is a value of N , say N_c , the solution of $V_{\text{eq}}(N) = V_c(N)$, at which the ETT happens at the equilibrium volume. Now, we shall use the fact that, at any N , $z[N, V_c(N)] = 0$ and integrate Eq. (11) from N_c to N . In the case in which $|N - N_c|/N_c \ll 1$, the coefficients γ , γ_c , λ , and λ_c can be considered constants and we obtain

$$z[N, V_{\text{eq}}(N)] = \pm(\gamma - \gamma_c)[V_{\text{eq}}(N) - V_c(N_c)] \pm(\lambda - \lambda_c)(N - N_c). \quad (17)$$

In a similar way, integrating Eq. (16), at fixed N , from $V_c(N)$ to V , one easily finds²

$$z(N, V) = \pm(\gamma - \gamma_c)[V - V_c(N)]. \quad (18)$$

Now, putting in the last equation $V = V_{\text{eq}}(N)$, and comparing with Eq. (17), we readily obtain the variation of V_c with the concentration,

$$\frac{dV_c}{dN} = -\frac{\lambda - \lambda_c}{\gamma - \gamma_c}. \quad (19)$$

In order to find a relationship between the variations of the concentration and the equilibrium volume, we have to minimize the free energy at fixed concentration. Since we are interested only in small deviations from the thermodynamic state $[N_c, V_c(N_c)]$, we may use only the more significant terms of the free-energy Taylor expansion about a generic equilibrium configuration, $[\bar{N}, V_{\text{eq}}(\bar{N})]$, with $|\bar{N} - N_c|/N_c \ll 1$,

$$F(T, V, N) = F[T, V_{\text{eq}}(\bar{N}), \bar{N}] + \frac{1}{2}[\kappa_T[V - V_{\text{eq}}(\bar{N})]^2 + 2\gamma[V - V_{\text{eq}}(\bar{N})] \times (N - \bar{N}) + \lambda(N - \bar{N})^2]. \quad (20)$$

In Eq. (20), all the thermodynamic derivatives, γ , λ , and the isothermal compressibility, $\kappa_T = \partial^2 F / \partial V^2$, are evaluated at the point $[\bar{N}, V_{\text{eq}}(\bar{N})]$. Thus, we obtain the variation of the equilibrium volume, which in the following shall be called charge compressibility:

$$\frac{dV_{\text{eq}}(N)}{dN} = -\frac{\lambda}{\gamma} = -\frac{\lambda_0 + \lambda_1}{\gamma_0 + \gamma_1}. \quad (21)$$

As stressed by the notation, it is convenient to consider separately the regular and special contributions to λ and γ , as follows from the separation of the free energy, $F = F_0 + F_1$. Thus, the ETT-related terms in Eq. (21) may be calculated by virtue of the theorem on small increments for thermodynamic potentials.⁷ This ensures that, in a vicinity of the ETT, $F_1 = \Omega_1$. Thus, using Eqs. (10), (12), and (17), we obtain

$$\gamma_1 = -(\gamma - \gamma_c)(\lambda - \lambda_c)\alpha|z|^{1/2}\Theta(z) \quad (22)$$

and

$$\lambda_1 = -(\lambda - \lambda_c)^2\alpha|z|^{1/2}\Theta(z). \quad (23)$$

Thus, at the lowest order in $|z|$, λ_1 and γ_1 are proportional to the special part of the DOS at the Fermi level,

$$\gamma_1 \cong -(\gamma_0 - \gamma_c)(\lambda_0 - \lambda_c)n_1(\mu), \quad (22')$$

$$\lambda_1 \cong -(\lambda_0 - \lambda_c)^2n_1(\mu) \quad (23')$$

and, therefore, the most significant contributions to Eq. (21) are given by

$$\frac{dV_{\text{eq}}(N)}{dN} \cong -\frac{\lambda_0}{\gamma_0} - \frac{\lambda_0}{\gamma_0} \left[\frac{\lambda_c}{\lambda_0} - \frac{\gamma_c}{\gamma_0} \right] (\lambda_0 - \lambda_c)n_1(\mu). \quad (21')$$

In the region $z < 0$, $n_1(\mu) = 0$ and dV_{eq}/dN may be considered constant. This gives for $V_{\text{eq}}(N)$ the linear behavior expected by Vegard's law. At $z = 0$, Eq. (21') indicates for the slope of $V_{\text{eq}}(N)$ a sudden variation proportional to the ETT-related DOS at the Fermi level, or to $|z|^{1/2}$. Interestingly, opposite to what was found for $V_{\text{eq}}(N)$, the slope of $V_c(N)$ does not exhibit any variation. In fact, from Eqs. (19), (22), and (23), we obtain, at any order in z ,

$$\frac{dV_c}{dN} = -\frac{\lambda_0 - \lambda_c}{\gamma_0 - \gamma_c}. \quad (19')$$

At this point, it is straightforward to apply the above method to the calculation of the ETT-related part of the isothermal compressibility, $\kappa_{T,1}$. The result, which was already derived in Ref. 3, is

$$\kappa_{T,1} = -(\gamma - \gamma_c)^2 n_1(\mu) \quad (24)$$

or, to the most significant order in $|z|$,

$$\kappa_{T,1} = -(\gamma_0 - \gamma_c)^2 n_1(\mu). \quad (24')$$

We would like to comment here that all the thermodynamical results quoted above were obtained using the fact that the special contribution to the thermodynamic potentials depends, at fixed temperature, only on the ETT order parameter z . Namely, our main ingredient here was the second derivative of the special grand potential with respect to the order parameter, which turns out to be proportional to special DOS. This shall be useful in Secs. II B and II C, where we shall generalize our scheme to include disorder scattering and finite temperatures, simply by introducing an appropriate complex order parameter. This, basically, will just allow the analytic continuation of Eq. (10). Thus, the second derivative of the grand potential will remain proportional to the special DOS, thus enabling us to recover on a more general ground, after some convenient renormalization, all the thermodynamical results quoted above.

B. Impure systems at $T=0$

In the present section, we shall extend the results of Sec. II A to the case in which impurity scattering is relevant, as it happens for random alloys. We shall give here the $T=0$ results, while the extension to finite temperatures shall be discussed in Sec. II C. In the present case quasiparticle lifetimes are finite, thus $\eta(\mathbf{p}) > 0$. Therefore, accordingly with Eq. (5), we shall integrate over the momentum space the contribution from the relevant band to the Bloch spectral function. This is done straightforwardly assuming $\eta(\mathbf{p}) = \eta[\mathbf{p}_c(\epsilon_c)]$, where $\mathbf{p}_c(\epsilon_c)$ is the momentum at which the relevant band has a stationary point. Since we are interested in only a proximity of the ETT and all the relevant states are in some neighborhood of \mathbf{p}_c and ϵ_c , our results will not be affected significantly by the assumption of a constant lifetime. In this way, we obtain a formula for the special part of the DOS that replaces Eq. (6)

$$n_1(z, \eta) = \alpha \operatorname{Re}\{\zeta^{1/2}\} = \frac{\alpha}{\sqrt{2}} [(z^2 + \eta^2)^{1/2} + z]^{1/2}, \quad (6')$$

where we have introduced the complex order parameter,

$$\zeta = \pm(E - \epsilon_c) + i\eta = z + i\eta. \quad (7')$$

The Riemann surface of $\zeta^{1/2}$ is determined by the condition, $\operatorname{Im}\{\zeta^{1/2}\} > 0$, which, in turn, implies that the special DOS, $n_1(z, \eta)$, has the same sing as the constant α . As is apparent from Eq. (6') and Fig. 2, the singularity already found in the $\eta=0$ theory is now smeared out and the special term in the DOS is analytic.

In order to make progress with the theory, it is necessary to neglect the dependence of the lifetimes on the en-

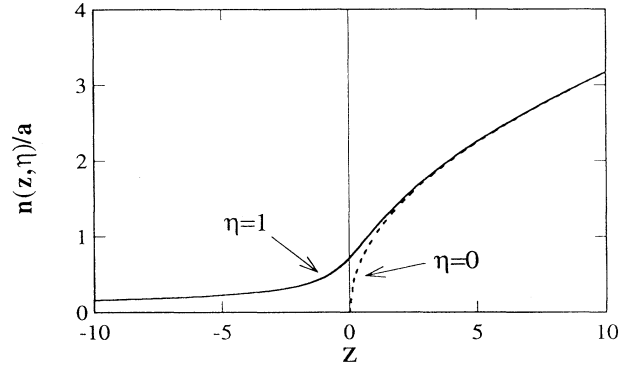


FIG. 2. The special part of the DOS, $n_1(z, \eta)$, vs the ETT order parameter z in the neighborhood of an ETT. Arbitrary units are used. Full line: $\eta=1$; dashed line: $\eta=0$ (i.e., no disorder broadening).

ergy. This is justified in the context of the Fermi-liquid theory, since the ETT-related properties are expected to depend appreciably only on electronic states close to the FS. Thus, a poor description of states far from the FS may contribute to energy integrated quantities only with additional, roughly linear in μ , terms. These, however, do not affect the second- and higher-order thermodynamic derivatives we are interested in.

Consistently with the above assumptions, we shall calculate the special part of the integrated DOS,

$$N_1(E, \eta) = \int_{-\infty}^E dE n_1(E, \eta), \quad (25)$$

without any care for the lower integration limit and obtain

$$\begin{aligned} N_1(z, \eta) &= \pm \frac{2\alpha}{3} \operatorname{Re}\{\zeta^{3/2}\} + \text{constant terms} \\ &= \frac{2n_1^3(z, \eta)}{3\alpha^2} (1 - 3 \tan^2 \varphi) + \text{constant terms}. \end{aligned} \quad (26)$$

In Eq. (26) we have introduced the phase φ , defined as follows:

$$\tan \varphi = \frac{\alpha^2 \eta}{2n_1^2(z, \eta)} = \left[\frac{n_1(0, \eta)}{n_1(z, \eta)} \right]^2 = \frac{\operatorname{Im}\{\zeta^{1/2}\}}{\operatorname{Re}\{\zeta^{1/2}\}}. \quad (27)$$

A further energy integration gives us the $T=0$ special part of the grand potential, namely,

$$\begin{aligned} \Omega_1(\mu, \eta) &= -\frac{4\alpha}{15} \operatorname{Re}\{\zeta^{5/2}\} + \text{terms linear in } z \\ &\quad + \text{constant terms} \\ &= -\frac{4n_1^5(z, \eta)}{15\alpha^4} (1 - 10 \tan^2 \varphi + 5 \tan^4 \varphi) \\ &\quad + \text{terms linear in } z + \text{constant terms}. \end{aligned} \quad (28)$$

In the limit of no impurity scattering, $\tan \varphi = 0$ and the above formulas reduce to the expressions discussed in the previous paragraph. Interestingly, the expected broadening due to impurity scattering enters in our expressions

only through the phase φ , which, for not too large values of η , is small for $z > 0$.

Interestingly, the analytic structure of Eq. (28) allows the repetition of the derivation of thermodynamic quantities along the lines of the previous paragraph. Indeed, under the assumption that η is independent of the chemical potential, as is justified in a neighborhood of an ETT, z and ξ are equivalent variables. Therefore the results given in Sec. II A, namely, Eqs. (19'), (21'), (22'), (23'), (24), and (24'), apply also to the present case, provided that $n_1(z)$ is replaced by $n_1(z, \eta)$. The only remark shall be that in the present, $\eta > 0$, case, the ETT-related corrections are no longer vanishing for $z < 0$, and that the previously found sudden variations in the slopes are smoothed accordingly.

C. Impure systems at $T > 0$

As we pointed out in the previous section, the inclusion of impurity scattering provides an analytic $T = 0$ expression for the special integrated DOS, Eq. (26). Thus, also finite temperature effects may be included analytically in the grand potential, via Eq. (9). Unfortunately, in our case, it is quite difficult to use the well-known low-temperature expansion¹³ of Eq. (9). We have found more convenient an alternative, nonperturbative, approach. For this purpose we shall use an exact result quoted in the Appendix, i.e., Eq. (A5). If we put there $J = \Omega_1(T, V, \mu)$ and $G(\varepsilon) = \Omega_1(\varepsilon)$, $g(\varepsilon) = -N_1(\varepsilon)$, and $g'(\varepsilon) = -n_1(\varepsilon)$ as given by Eqs. (6'), (25), and (28), respectively, we readily obtain

$$\Omega_1(T, V, \mu) = \Omega_1(T=0, V, \mu) + a \operatorname{Re} \left\{ \int_0^\infty dx \sum_{m=1}^{\infty} (-1)^m \frac{k_B T}{m} e^{-mx/k_B T} \times [(\xi \pm x)^{1/2} + (\xi \mp x)^{1/2}] \right\}, \quad (29a)$$

where

$$\xi = \pm(\mu - \varepsilon_c) + i\eta \quad (29b)$$

and where the lower or upper sign correspond to those given in Eqs. (3). The integrals in Eq. (29a) are related to the incomplete Γ function. However, in their evaluation, it is necessary to pay some attention in order to choose the appropriate Riemann surfaces for the square roots, accordingly with the discussion of Sec. II B. With this care, we obtain

$$\Omega_1(T, V, \mu) = \operatorname{Re} \left\{ -\frac{4a}{15} \xi^{5/2} [1 + \Phi(\Theta)] \right\}, \quad (30)$$

where we have introduced the effective complex dimensionless "temperature"

$$\Theta = k_B T / \xi \quad (30a)$$

and where the "broadening" function,

$$\Phi(\Theta) = -\frac{15}{4} \sum_{m=1}^{\infty} (-1)^m F \left[\frac{m}{\Theta} \right] \quad (30b)$$

is defined in terms of the incomplete Γ function, which enters in $F(x)$ in the following way:

$$F(x) = x^{-5/2} [e^x \Gamma(3/2, x) + i e^{-x} \Gamma(3/2, -x)]. \quad (30c)$$

In the present form, Eq. (30), the "special" grand potential appears as the sum of its $T = 0$ limit and a correction term proportional to $\Phi(\Theta)$. As shown in Fig. 3, these corrections are relevant only in a proximity of an ETT whose size is comparable with $k_B T$.

Although Eq. (30) is exact as it stands, some physical insights may be obtained by studying its asymptotic

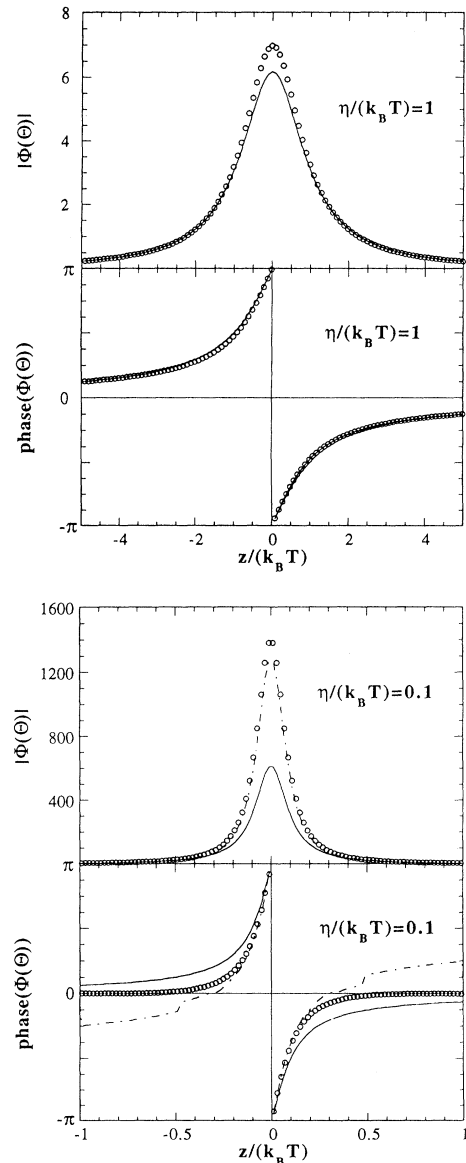


FIG. 3. The absolute values and the phases of the broadening function $\Phi(\Theta)$, $\Theta = k_B T / (z + i\eta)$, defined in Eq. (34) are plotted vs the dimensionless ratio $z/k_B T$ for two different values of $\eta/k_B T$. Circles: numerical estimates; full line: asymptotic formula for $\Theta < 1$ [Eq. (32)]; dashed line: asymptotic formula for $\Theta > 1$ [Eq. (32')].

behaviors. Using well-known results for the incomplete Γ function¹⁴ in both the large and small x regimes, we obtain that the more significant contributions to $F(x)$ are the following:

$$F(X) \cong \frac{\sqrt{\pi}}{2} (1+i)x^{-5/2} + O(|x|^{-3/2}) \quad \text{for } |x| < 1 \quad (31a)$$

and

$$F(x) \cong 2x^{-2} + O(|x|^{-4}) \quad \text{for } |x| > 1. \quad (31b)$$

In order to have asymptotic estimates of the broadening function $\Phi(\Theta)$, we need now to distinguish between two different circumstances. Let us consider first the case $|\Theta| < 1$, that is to say $k_B T < |\xi|$. In this situation *all* the terms in the sum of Eq. (30b) may be approximated by Eq. (31b) and summed over to obtain

$$\Phi(\Theta) = \frac{15}{4} \frac{\pi^2}{6} \Theta^2 + O(|\Theta|^4) \quad \text{for } |\Theta| < 1, \quad (32)$$

which, once inserted in Eq. (30), using also Eq. (6'), gives

$$\Omega_1(T, V, \mu) - \Omega_1(T=0, V, \mu) \cong -\frac{\pi^2}{6} (k_B T)^2 n_1(z, \eta), \quad (33)$$

which could have been obtained using the standard technique for the evaluation of integrals of the type of Eq. (9) in the low-temperature limit.¹³ In the present case, however, Eq. (33) holds under the much broader assumption $|\Theta| < 1$. In other words, the "low-temperature limit," Eq. (33), could be realized even at relatively high temperatures, provided the ETT order parameter, ξ , is large, as it happens if the relevant states are largely broadened by disorder.

In the opposite, $|\Theta| > 1$ or $k_B T > |\xi|$, case, if we call M the largest integer smaller than $|\Theta|$, the sum (30b) is conveniently rewritten as follows:

$$\Phi(\Theta) = -\frac{15}{4} \left[\sum_{m=1}^M (-1)^m F \left[\frac{m}{\Theta} \right] + \sum_{m=M+1}^{\infty} (-1)^m F \left[\frac{m}{\Theta} \right] \right]. \quad (34)$$

Applying to Eq. (34) the appropriate asymptotic formulas for $F(x)$, i.e., Eqs. (31a) or (31b), we obtain, at the leading orders, contributions proportional to $\Theta^{5/2}$ and to Θ^2 ,

$$\Phi(\Theta) \cong -\frac{15}{4} [(1+i)c_1(M)\Theta^{5/2} + c_2(M)\Theta^2] + O(|\Theta|^{3/2}) \quad \text{for } |\Theta| > 1, \quad (32')$$

where we have introduced the coefficients

$$c_1(M) = \frac{\sqrt{\pi}}{2} \sum_{m=1}^M \frac{(-1)^m}{m^{5/2}}$$

and

$$c_2(M) = 2 \sum_{m=M+1}^{\infty} \frac{(-1)^{m+1}}{m^2} = -\frac{\pi^2}{6} + 2 \sum_{m=1}^M \frac{(-1)^{m+1}}{m^2}.$$

Accordingly, the correction term for the grand potential shall be

$$\Omega_1(T, V, \mu) - \Omega_1(T=0, V, \mu) \cong a c_1(M) (k_B T)^{5/2} + c_2(M) (k_B T)^2 n_1(z, \eta). \quad (33')$$

We wish to remark that the limit $|\Theta| > 1$ could not be easily observable in a random alloy. In fact, it could be obtained only in a vicinity of an ETT and for quite high temperatures, $k_B T > \eta$. Under these circumstances lattice excitations would be relevant and could not allow us to detect the contribution to the specific heat proportional to $T^{1/2}$, which is expected to arise from the $T^{5/2}$ term in Eq. (33').

As discussed in Secs. II A and II B, the calculation of the equilibrium volume at a given concentration, $V_{\text{eq}}(N)$, involves the second ξ derivatives of the excess grand potential, which in the present case is given by Eq. (30). Interestingly, as is evident from Eq. (33'), no contributions to the above derivatives arise from possible terms proportional to $\Theta^{5/2}$ in the expansion of $\Phi(\Theta)$. Therefore, in *both* the limits $|\Theta| < 1$ and $|\Theta| > 1$, the leading contributions to $\partial^2 \Omega_1 / \partial^2 \xi$ come from the term proportional to Θ^2 . Namely, we find

$$\partial^2 \Omega_1 / \partial^2 \xi = -\bar{n}_1(z, \eta; T) \quad (35a)$$

where

$$\bar{n}_1(z, \eta; T) = n_1(z, \eta) \left[1 + \frac{a^4 c_2}{4} \left[\frac{k_B T}{n_1^2(z, \eta)} \right]^2 \times (4 \cos^2 \varphi - 3) \cos^4 \varphi \right]. \quad (35b)$$

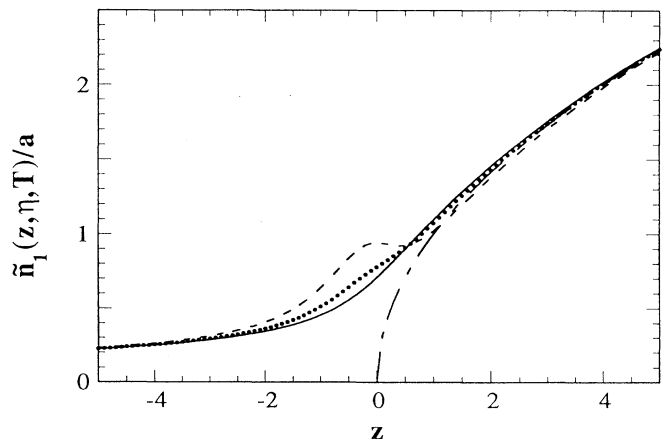


FIG. 4. The "renormalized" DOS defined in Eq. (35a), $\bar{n}_1(z, \eta, T)$, is plotted vs z in arbitrary units. Dashed line: $\eta=1$ and $k_B T=0.9$; dotted line: $\eta=1$ and $k_B T=0.5$; continuous line $\eta=1$ and $k_B T=0$; dash-dotted line: $\eta=0$ and $k_B T=0$. Remarkably, up to relatively large values of $k_B T/\eta$, the effect of temperature consists only in a modest broadening with respect to the $T=0$ curve.

Therefore the renormalized T -dependent DOS, $\bar{n}_1(z, \eta; T)$, will enter in our expressions, Eqs. (19') and (21'), for dV_c/dN and dV_{eq}/dN in the place of $n_1(z)$. As we show in Fig. 4 where $\bar{n}_1(z, \eta; T)$ is plotted, the effect of the temperature consists in an additional smearing of the Van Hove singularity. However, these effects are not large for $k_B T/\eta \lesssim 0.5$, and therefore, at least for many alloy systems, they should not have deleterious consequences on the possibility of observing the ETT-related deviations from linearity in $V_{eq}(N)$.

III. LATTICE PARAMETER AND TOTAL ENERGIES VERSUS CONCENTRATION IN THE Ag-Pd SYSTEM

In this section we are going to discuss, also in comparison with numerical calculations and measurements for the AgPd system, the results we derived in Sec. II for the variations of the alloy equilibrium volumes and the thermodynamic potentials as a function of the concentration. AgPd alloys have a continuous fcc solid solution phase in all the range of concentrations, and, as discussed in Paper II, constitute a very interesting test system. In fact, on varying the e/a ratio from 10 (pure Pd) to 11 (pure Ag), five distinct ETT's are encountered.

The starting point of our present discussion shall be Eq. (21), where the charge compressibility, dV_{eq}/dN , was expressed in terms of the thermodynamic derivatives γ and λ . These, in turn, are related through Eqs. (14) and (15) to the DOS derivatives with respect to the unit-cell volume and the e/a ratio. Far from ETT's, as we argued in Sec. II A, λ and γ are nearly constant. Thus, in those concentration ranges in which no ETT is encountered, the unit-cell equilibrium volume is linear versus e/a , or, in other words, Vegard's rule is satisfied. In the neighborhood of an ETT, however, the nonlinear contributions λ_1 and γ_1 , proportional to the special DOS, n_1 , must also be included. Thus, on varying the e/a ratio in a random alloy system, we expect dV_{eq}/dN to be nearly constant

until we get close to an ETT, and then to change quite rapidly in the ETT proximity. Eventually, when the ETT region is crossed over, the charge compressibility will approach some different, nearly constant, value. Therefore, at $T=0$ and neglecting the effects of substitutional disorder, deviations of the lattice constant from the linearity predicted by Vegard's law could be associated with the occurrence of changes in the FS topology. Clearly, accordingly with the theory of the previous section, finite temperatures and substitutional disorder smear out the singularity in n_1 . This notwithstanding, as long as the temperature remains reasonably low and the quasiparticle lifetimes not too short, such a broadening could not hide the relatively sudden changes we expect for the lattice constant trends.

In order to make the above argument more explicit, we have estimated the charge compressibility within the rigid band model (RBM) of Mott and Jones.¹⁵ As is well known, the RBM assumes that, on alloying, the band shape does not vary, whereas the Fermi level is raised, accordingly with the band filling. Thus, in spite of its simplicity, this model incorporates much of the physics of the problem; i.e., it is able to deal reasonably well with the e/a ratio, which, in turn, is deeply related to the ETT order parameter z . Of course, RBM estimates of the critical concentrations at which ETT's occur could not be accurate,⁴ nevertheless the changes in the FS topology are described quite satisfactorily and we should be able to obtain within the model a reasonable, at least qualitative, picture of the phenomenology connected with the ETT's. Moreover, as we argue in Paper II, the ETT's in AgPd alloys, a typical split band system, can be described quite carefully in a RBM scheme. RBM estimates of ETT critical concentrations are actually quite accurate, as shown in Table I, where they are compared with those from our KKR-CPA calculations.

A RBM estimate for λ is easily obtained. In fact, if we consider the DOS's at two different e/a ratios, N and $N + \Delta N$, we have

$$n[E - \mu(N + \Delta N)] - n[E - \mu(N)] = \left[\frac{\partial n(E - \mu)}{\partial N} \right]_V \left[\frac{\partial \mu}{\partial N} \right]_V \Delta N = \lambda \left[\frac{\partial n(E - \mu)}{\partial N} \right]_V \Delta N, \quad (36)$$

TABLE I. List of the ETT's occurring in the AgPd alloy system. For each we report the critical concentration, as estimated from RBM and *ab initio* KKR-CPA calculations (Ref. 5), the corresponding type of Van Hove singularity in the spectrum, the reciprocal space vector at which the transitions occur, and the signs of the derivatives of the relevant special DOS and ETT order parameter. Here $S1$, $S2$, m , and M stand for saddle point of index 1, saddle point of index 2, minimum, and maximum, respectively. Although not relevant for the AgPd system, the values corresponding to an ETT due to a minimum in the spectrum are also reported.

ETT	Critical concentrations		Type	Relevant		
	RBM	KKR-CPA		k -space point	$\text{sgn}(dn_1/dN)$	$\text{sgn}(dz/dN)$
1	10.06	10.06	$S1$	$\sim(0.39, 0.39, 0.47)$	-	+
2	10.13	10.20	M	L	-	-
3	10.33	10.35	M	X	-	-
4	10.53	10.53	M	X	-	-
5	10.64	10.70	$S2$	L	+	-
			m		+	+

where, as is natural in the framework of Landau's Fermi-liquid theory, the energies are measured from the Fermi level. Then, inserting in Eq. (15) the expression for $[dn(E)/dN]_V$ which follows from Eq. (36) and integrating over the energy, we find

$$\lambda = 1/[2n(\mu)] .$$

Thus, from Eqs. (21) and (14), we obtain an expression for the charge compressibility suitable for numerical computation,

$$\frac{dV_{\text{eq}}^{\text{RBM}}(N)}{dN} = \frac{1}{2} \left[\int_{-\infty}^{\mu(N)} dE \left(\frac{\partial n(E)}{\partial V} \right)_N \right]^{-1} . \quad (37)$$

At this point, in order to have a more immediate understanding of the implications of Eq. (37), it is convenient to write the alloy equilibrium volume V_{eq} as the sum of a regular and ETT-related terms, $V_{\text{eq}} = V_{\text{eq}}^0 + V_{\text{eq}}^{1,(i)}$. Here $V_{\text{eq}}^{1,(i)}$ is originated by the i th ETT, and, therefore, it is proportional to the corresponding special DOS $n_1^{(i)}(z^{(i)})$ and relevant only in the proximity of the same ETT. Moreover, we assume $|V_{\text{eq}}^{1,(i)}/V_{\text{eq}}^0| \ll 1$. Thus, using Eqs. (11) and (7), we rewrite Eq. (21') as

$$\frac{dV_{\text{eq}}^0(N)}{dN} \cong -\frac{\lambda_0}{\gamma_0} , \quad (38)$$

with λ_0/γ_0 constant in each of the intervals between different ETT's, and

$$\begin{aligned} \frac{dV_{\text{eq}}^1(N)}{dN} &\cong -\frac{\lambda_0}{\gamma_0} \left[\frac{\lambda_c}{\lambda_0} - \frac{\gamma_c}{\gamma_0} \right] (\lambda_0 - \lambda_c) n_1^{(i)}(z^{(i)}(N)) \\ &\cong \frac{dV_{\text{eq}}^0(N)}{dN} \left[\frac{\lambda_c}{\lambda_0} - \frac{\gamma_c}{\gamma_0} \right] (\lambda_0 - \lambda_c) n_1^{(i)}[z^{(i)}(N)] \\ &\cong -\frac{dV_{\text{eq}}^0(N)}{dN} \frac{d(\mu - \varepsilon_c)}{dN} \\ &\quad \times (1 - \lambda_c/\lambda_0) n_1^{(i)}[z^{(i)}(N)] . \end{aligned} \quad (38')$$

Now, within the RBM $d\varepsilon_c/dN \approx \lambda_c = 0$, thus, in correspondence to each of the ETT's, we have an estimate for the size of dV_{eq}^1/dN :

$$\frac{dV_{\text{eq}}^1(N)}{dN} \cong -\frac{dV_{\text{eq}}^0(N)}{dN} \frac{d\mu}{dN} n_1^{(i)}[z^{(i)}(N)] . \quad (38'')$$

In the case we are interested in, according to our relativistic local-density-approximation (LDA) KKR-CPA calculations (paper II), $a_{\text{Pd}} = 3.889 \text{ \AA}$ and $a_{\text{Ag}} = 4.041 \text{ \AA}$, while the Fermi energy obviously increases with e/a . These estimates for the lattice parameters compare favorably both with x-ray measurements,¹⁰ $a_{\text{Pd}} = 3.883 \text{ \AA}$ and $a_{\text{Ag}} = 4.077 \text{ \AA}$, and with theoretical calculations from other groups,¹⁶ $a_{\text{Pd}} = 3.848 \text{ \AA}$ and $a_{\text{Ag}} = 4.008 \text{ \AA}$. Thus, for the AgPd system, $\text{sgn}([dV_{\text{eq}}^0(N)/dN]d\mu/dN) > 0$. Therefore, as we see from Eqs. (38''), the ETT-related contributions to the charge compressibility, dV_{eq}^1/dN , are proportional, as expected, to the special DOS's or, in other words, to the "strengths" of their corresponding

Van Hove singularities in a DOS plot. As is determined only by the special contributions, we shall find it convenient in what follows to calculate the sign of the first derivative of the charge compressibility. This, in general, is given by

$$\text{sgn} \left[\frac{d^2 V_{\text{eq}}(N)}{dN^2} \right] \cong -\text{sgn} \left[\frac{dV_{\text{eq}}^0(N)}{dN} \frac{d\mu}{dN} \right] \text{sgn} \left[\frac{dn_1^{(i)}}{dN} \right] , \quad (39)$$

and thus, for AgPd alloys, it is just the opposite of $\text{sgn}(dn_1^{(i)}/dN)$. The last quantity, which is easily calculated from Eqs. (6) and (7) or just from a look to Fig. 1, is shown in Table I for each kind of Van Hove singularity.

We evaluated numerically Eq. (37) using the pure Pd DOS from our first principle KKR-CPA calculations (Paper II) at two different lattice parameters, close to the equilibrium value, 3.884 and 3.889 \AA , respectively.¹⁷ Our results for dV_{eq}/dN and for the DOS are plotted in Fig. 5 versus the RBM e/a . In the same figure the vertical lines mark the RBM predictions for the critical concentrations corresponding to the FS topology changes found in AgPd

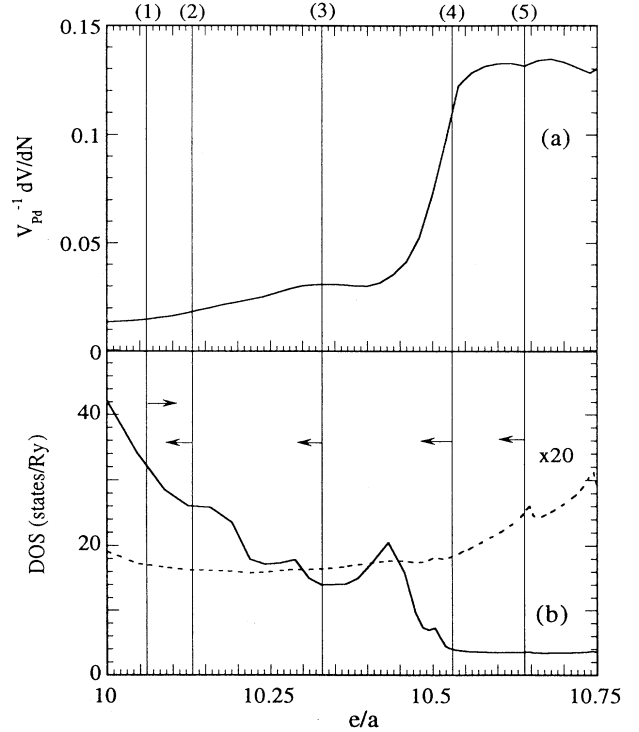


FIG. 5. (a) RBM charge compressibility, $V_{\text{Pd}}^{-1} dV/dN$, vs the e/a ratio in AgPd alloys. Vertical lines identify the RBM estimates for the different ETT's found in AgPd (Ref. 5 and Table I). The numbers marked on the top individuate each transition and correspond to the classification given in Table I. (b) Pd DOS plotted vs the RBM e/a . Solid line: total DOS; dashed line: s - p DOS (note the magnification). Vertical lines have the same meaning as in (a) and the arrows indicate, for each ETT, the direction $z > 0$ along which the order parameter increases. According with Eq. (6), the special DOS in absence of substitutional disorder is nonvanishing only for $z > 0$.

(see Paper II). These ETT's are listed and classified in Table I. In the same Fig. 5(b), accordingly with the convention stated in Eq. (7), the arrows indicate the directions in which the ETT order parameter z is positive or, in other words, where the special DOS is nonvanishing. In the following we shall analyze in detail, on the basis of Fig. 5 and Table I, each of the above ETT's in the AgPd system.

(1) At $e/a = 10.06$ we have the first ETT due to the disruption of a neck at $q \sim (0.39, 0.39, 0.47)\pi/a$. Following the classification of Sec. II A, it corresponds to a saddle point of index 1 ($S1$) in the band structure, thus the special contribution to the DOS should be negative and nonvanishing in the direction of increasing e/a . Therefore, accordingly with Eq. (39), $d^2V_{\text{eq}}/dN^2 > 0$ and we have an increment of the charge compressibility for $e/a \gtrsim 10.06$.

(2) A second ETT occurs at $e/a = 10.13$, due to the presence of a band maximum at the L point, and generates a positive special contribution n_1 in the range $e/a \lesssim 10.13$, clearly visible in Fig. 5(b). This implies an increment of dV_{eq}/dN , which is apparent in Fig. 5(a) in the above concentration range. Since the ETT's (1) and (2) are very close to each other and both give rise to contributions of the same sign, we cannot estimate their relative importance.

(3) At $e/a = 10.33$ we have a third ETT related to a band maximum at the X point. Thus, for $e/a \lesssim 10.33$, the corresponding special DOS and the charge compressibility exhibit the same trends as in (2).

(4) At $e/a = 10.53$, as the d bands get filled, we find a fourth ETT with a very large effect on the DOS, again due to a band maximum at the X point. This ETT contributes to the DOS and dV_{eq}/dN as in (2), for $e/a \lesssim 10.53$.

(5) A neck opens at L as the Fermi level crosses a saddle point of index 2 ($S2$) in the band structure ($e/a = 10.64$). Here the contribution to n_1 is negative and causes a decrease of the charge compressibility in the range $e/a \lesssim 10.64$. However, this effect is related to a very weak singularity in the s and p DOS components, as we show, on a magnified scale, in Fig. 5(b). Therefore, only a small effect on dV_{eq}/dN is visible in Fig. 5(a).

The above analysis appears to confirm the picture we have drawn at the beginning of this section for the variations of the alloy unit-cell equilibrium volume. However, due to the overlapping of several distinct ETT's contributing in the same direction, we find only two concentration ranges in which dV_{eq}/dN is nearly constant, namely, about $e/a \sim 10.4$ and $e/a > 10.65$. As is apparent from Fig. 5(a), the largest effect occurs as the d states get filled, or, as discussed in Paper II, at the transition to a single sheet, simply connected, "simple-metal-like," Fermi surface.

Once dV_{eq}/dN is integrated over, our rigid band model easily gives the equilibrium unit-cell volume as a function of the atomic concentrations. Here, as is customary in alloy physics, we prefer to discuss in terms of the lattice parameter, $a_{\text{eq}} = (V_{\text{eq}}/4)^{1/3}$. In Fig. 6(a) we have plotted the deviations of this quantity from Vegard's rule, in for-

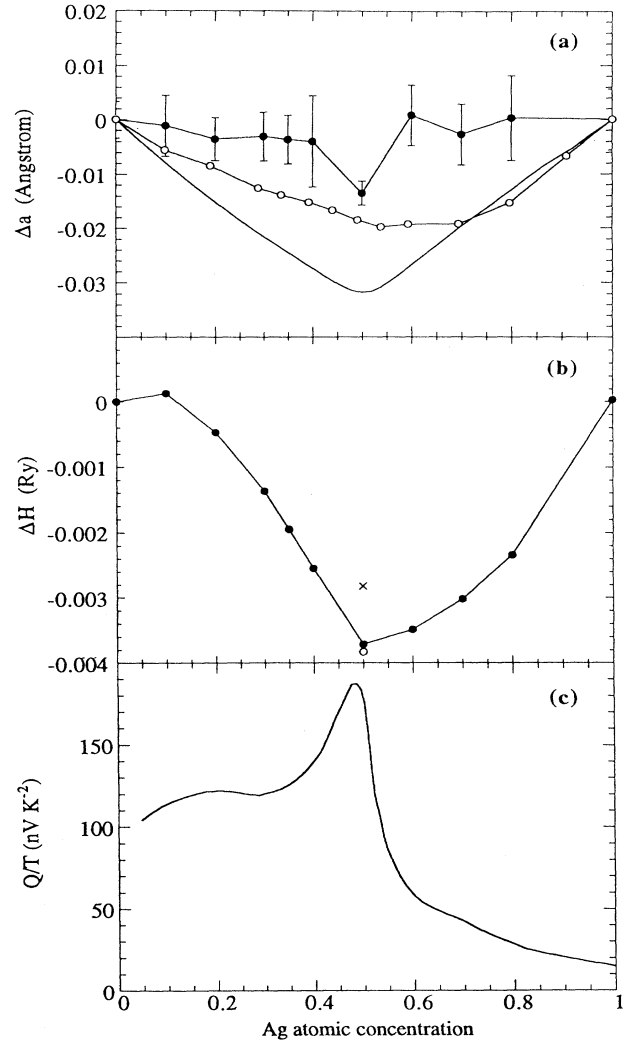


FIG. 6. (a) Deviations of the lattice parameters in from Vegard's rule, Δa [Eq. (40)], for AgPd alloys. Full circles with error bars: *ab initio* KKR-CPA calculations (Ref. 5); open circles: x-ray measurements (Ref. 10); full line: RBM (see Sec. III). (b) $T = 0$ mixing enthalpies, ΔH [Eq. (41)] for the same system. Full circles: *ab initio* KKR-CPA calculations (Ref. 5) (estimated errors have the same size of the symbols); open circle: experiment (Ref. 19); cross: total-energy calculations by Lu *et al.* (Ref. 16). (c) Measured (Ref. 11) thermoelectric power Q as a function of the Ag concentration in AgPd alloys.

mulas,

$$\Delta a = a_{\text{eq}}(c) - [ca_{\text{eq,Ag}} - (1-c)a_{\text{eq,Pd}}], \quad (40)$$

where c is the Ag atomic concentration. As is apparent, our simple model compares quite favorably with room-temperature experiments.¹⁰ In fact, the overall trends are well reproduced, while the largest deviation is overestimated of about 50% and its position moved toward lower concentrations with respect to the experiment. However, finite temperatures and lifetimes, not included in our RBM calculations,¹⁷ are expected to smooth the

sudden variations found for the RBM charge compressibility. Moreover, as found in Sec. II A, the presence of finite lifetimes causes the special DOS to be nonvanishing on *both* sides of an ETT. Thus, the substitutional disorder could move the effects of the largest contribution to the charge compressibility toward higher Ag concentrations. As noted above, this contribution is related to the fourth ETT at $e/a = 10.53$, and roughly corresponds to the RBM minimum for Δa . Interestingly, the fine effects due to other ETT's, while clearly visible in our plot of dV_{eq}/dN [Fig. 5(a)] appear to be washed out after the integration. We would like to stress that this fact has nothing to do with the temperature or the substitutional disorder and suggests that only the effects of "strong" ETT's could be observed in lattice constant measurements.

In Fig. 6(a), we report also our KKR-CPA results for the same system (see Paper II). These calculations include a corrective term to the Madelung energy in order to account for charge correlation effects (Paper II, and references therein). Also in this case the trends appear to be substantially reproduced; nevertheless, the comparison is now more difficult. Within a first-principles scheme, in fact, the lattice parameter a is calculated, at each concentration, as the position of the minimum of the total energy versus a . Unfortunately, these minima are very flat. Therefore, while we are able to obtain accurate values for the total energies or the mixing enthalpies [see Fig. 6(b)], our estimates of a_{eq} are affected by errors that are relevant on the very fine scale of the variations of Δa . In this situation the structures visible in the plot of the KKR-CPA Δa cannot be considered significant and the only feature that appears relevant is an overall underestimate of Δa . The source of this is probably related to the way in which a mean-field approximation, as the CPA is, deals with disorder. We think that fluctuations, namely, those inducing local order, could cause quasiparticle lifetimes larger than those obtained from a mean-field theory. On the other hand, the RBM, which uses DOS's produced from KKR calculations for pure Pd, lies on the same kind of basic physical approximation, namely, the LDA. In our opinion, therefore, the more significant difference with respect to the KKR-CPA is that RBM assumes infinite lifetimes.¹⁷ The fact the RBM overestimates Δa supports the above interpretation of CPA results.

We would like to conclude this section with some remarks about two other quantities, the enthalpy of mixing and the thermoelectric power in AgPd alloys. The former, plotted versus the concentration in Fig. 6(b), was evaluated from our KKR-CPA calculations (see Paper II) at $T=0$, accordingly with the formula

$$\Delta H(c) = E_{\text{TOT}}(c) - [cE_{\text{TOT,Ag}} - (1-c)E_{\text{TOT,Pd}}]. \quad (41)$$

Evidently, by virtue of Landau's theorem on small increments for thermodynamic potentials, the ETT-related contributions to the mixing enthalpy coincide, at the lowest order in n_1 , with the special parts of the grand potential and, therefore, can be estimated from Eq. (10). Thus, these contributions are expected to have a sign opposite to the constant α of Eq. (8), i.e., positive for saddle

points and negative for maxima and minima in the band structure. Indeed, we observe in Fig. 6(b) a small region, $0.05 \lesssim e/a \lesssim 0.10$, in which ΔH is slightly positive. This could be associated to the saddle point encountered in the first ETT. In the present case, however, the ETT-related contributions are particularly small, since they are proportional to n_1^5 , while the regular terms, although smooth, are large and not expected to be linear with the concentration. Therefore, we cannot say anything definitive about the quantitative influences of ETT's on the mixing enthalpies.

It is interesting to check against what we argued on the basis of the trends of the lattice parameters and mixing enthalpies, the thermoelectric power measurements for the same AgPd alloy system.¹¹ As is well known, in a $T=0$ theory and in the absence of disorder, these quantities should diverge as $|z|^{-1/2}$ or $n_1^{-1}(z)$ in a neighborhood of an ETT,¹ while finite temperatures and lifetimes turn the divergences in finite peaks, whose broadening is related to T and η .^{2,3} It is thus natural to interpret the sharp peak at $e/a \sim 10.5$ as due to the fourth ETT corresponding to the filling of d bands. This interpretation is consistent also with the theoretical thermopower calculations by Butler and Stocks.¹⁸ Unfortunately there are no measurements at very low Ag concentration, thus the plot in Fig. 6(c) cannot help in the discussion of the first ETT at $c \sim 0.05$. However, quite remarkably, the extended plateau region in the range $c \gtrsim 0.20$, in the light of the above discussion, could be interpreted as the sum of two distinct contributions merged together and related, respectively, to the ETT's 2 and 3, which according with our KKR-CPA calculations should occur at $c = 0.20$ and $c = 0.35$. It would be interesting to test this point. One possible way could be to repeat the thermopower measurements at different temperatures. In summary, also the thermopower measurements appear to support our view that the ETT's connected with "strong" Van Hove singularities, like (4), may lead to observable effects, while it is much more difficult to evidenciate weaker ETT's.

IV. CONCLUSIONS

In the present paper we have extended Lifshitz's theory of electronic topological transitions including the effects of finite temperatures and quasiparticle lifetimes. This was formally accomplished via the introduction of a complex order parameter, whose imaginary part is proportional to the inverse quasiparticle lifetimes. In this way we have found an analytic continuation of Lifshitz's theory. This framework allowed us to deal with finite temperatures through the introduction of an appropriate complex broadening function whose dependence on the dimensionless ratio between the temperature and the ETT complex order parameter was investigated in different asymptotic regimes. The principal result of the above theory was a general expression, Eq. (30), for the special, or ETT-related, part of the grand potential, exact in the neighborhood of an ETT. Moreover, we have analyzed the dependence of the equilibrium volumes on the (valence) electron per atom ratio (e/a) in metallic random alloys. Namely, we have found that, whenever these

systems undergo changes of their Fermi-surface topology on approaching the ETT critical concentrations the lattice parameter deviates from the behavior linear with e/a predicted by Vegard's rule. These deviations are related to the special part of the DOS at the Fermi level, $n_1(\mu)$.

Our analysis of the influence of ETT's on macroscopic properties of alloy systems was confirmed by the study of a real system, AgPd, for which LDA-KKR-CPA determinations of the lattice parameters and mixing enthalpies are presented. These calculations are in good agreement with the experiments and with a simplified rigid band model version of our theory for the variations of the alloy equilibrium volume versus e/a . Interestingly, the largest deviations from Vegard's law found for the AgPd lattice parameters ($e/a \sim 10.5$) can be associated with the ETT due to the filling of the d bands. In fact, on increasing the Ag concentration beyond the above value the alloy Fermi surface undergoes a transition toward a simple-metal-like topology, with only a simply connected structure all contained in the first Brillouin zone. The other ETT's found in these alloys give rise to small special contributions to the DOS. Thus, their effects, while evident in a plot of what we called charge compressibility, are hardly distinguishable in lattice parameter measurements. This view is supported also by the comparison with thermoelectric power measurements. In fact, $e/a \sim 10.5$ corresponds to the largest peak in a plot of this quantity versus the alloy concentration. The plateau that is evident in the low Ag concentrations region of the same plot could be explained as the sum of several broad peaks due to the ETT's with small effects on the DOS.

Our results on AgPd show that, opposite to the RBM model, the coherent potential approximation underestimates of lattice parameter deviations from Vegard's rule. We argued in Sec. III that this fact could be due to a systematic underestimation of the quasiparticle lifetimes related to the mean-field nature of the CPA theory. Our detailed LDA-KKR-CPA study of the AgPd Fermi surfaces and their topologies is presented in Paper II.

ACKNOWLEDGEMENTS

We wish to acknowledge financial support from the Istituto Nazionale di Fisica della Materia (INFN), the Ministero per l'Università e Ricerca Scientifica (MURST), and the HCM Ψ_k network.

APPENDIX

In this appendix we shall evaluate the integral

$$J = \int_{-\infty}^{+\infty} d\varepsilon f(\varepsilon - \mu) g(\varepsilon), \quad (\text{A1})$$

where $g(\varepsilon)$ is an analytic function of the energy and $f(x) = (1 + e^{x/k_B T})^{-1}$ is the Fermi function. Moreover we assume that $\lim_{\varepsilon \rightarrow -\infty} g(\varepsilon) = 0$ and $g(\varepsilon)$ is well behaved as $\varepsilon \rightarrow +\infty$.

Integrating Eq. (A1) by parts, changing the integration variable to $x = \varepsilon - \mu$ and performing some other straightforward manipulation we obtain

$$J = \frac{1}{k_B T} \int_0^{+\infty} dx \frac{e^{-x/k_B T}}{(1 + e^{-x/k_B T})^2} [G(\mu + x) + G(\mu - x)], \quad (\text{A2})$$

where $G(\varepsilon) = \int_{-\infty}^{\varepsilon} dx g(x)$.

At this point it is convenient to expand the Fermi function derivative in powers of $e^{-x/k_B T}$. Remarkably the series so obtained,

$$\frac{-e^{-x/k_B T}}{(1 + e^{-x/k_B T})^2} = \frac{1}{k_B T} \sum_{m=1}^{\infty} (-1)^m m e^{-mx/k_B T} \quad (\text{A3})$$

is convergent within the domain of integration at any temperature. In order to proceed further we insert the series (A3) in Eq. (A2), integrate twice by parts and obtain

$$J = - \lim_{x \rightarrow 0^+} \left[[G(\mu + x) + G(\mu - x)] \sum_{m=1}^{\infty} (-e^{-x/k_B T})^m + k_B T [g(\mu + x) - g(\mu - x)] \sum_{m=1}^{\infty} \frac{(-e^{-x/k_B T})^m}{m} \right] - k_B T \int_0^{+\infty} dx [g'(\mu + x) + g'(\mu - x)] \sum_{m=1}^{\infty} \frac{(-e^{-x/k_B T})^m}{m}. \quad (\text{A4})$$

In Eq. (A4) the sums have to be evaluated before the limit. In this way we obtain two formulas useful in the evaluation of integrals of the kind of Eq. (A1), namely,

$$J = G(\mu) - k_B T \int_0^{+\infty} dx [g'(\mu + x) + g'(\mu - x)] \times \sum_{m=1}^{\infty} \frac{(-e^{-x/k_B T})^m}{m} \quad (\text{A5})$$

and

$$J = G(\mu) + k_B T \int_0^{+\infty} dx [g'(\mu + x) + g'(\mu - x)] \times \ln(1 + e^{-x/k_B T}). \quad (\text{A6})$$

- ¹I. M. Lifshitz, Zh. Eksp. Teor. Fiz. **33**, 1569 (1960) [Sov. Phys. JETP **11**, 1130 (1960)].
- ²A. A. Varlamov, V. S. Egorov, and A. V. Pantsulaya, Adv. Phys. **38**, 469 (1989).
- ³Ya. M. Blanter, M. I. Kaganov, A. V. Pantsulaya, and A. A. Varlamov, Phys. Rep. **245**, 160 (1994).
- ⁴E. Bruno, B. Ginatempo, E. S. Giuliano, A. V. Ruban, and Yu. Kh. Vekilov, Phys. Rep. **249**, 353 (1994).
- ⁵E. Bruno, B. Ginatempo, and E. S. Giuliano, following paper, Phys. Rev. B **52**, 14 557 (1995).
- ⁶L. D. Landau, Zh. Eksp. Teor. Fiz. **30**, 1058 (1956) [Sov. Phys. JETP **3**, 920 (1956-57)].
- ⁷L. D. Landau and I. M. Lifshitz, *Statistical Physics* (Pergamon, Oxford, 1980), Pt. I.
- ⁸A. A. Abrikosov, *Fundamental of the Theory of Metals* (North-Holland, Amsterdam, 1988).
- ⁹L. Van Hove, Phys. Rev. **89**, 1189 (1953).
- ¹⁰W. B. Pearson, *A Handbook of Lattice Spacings and Structures of Metals and Alloys* (Pergamon, Oxford, 1958).
- ¹¹A. M. Guènauld, Philos. Mag. **30**, 641 (1974).
- ¹²R. C. Casella, Phys. Rev. Lett. **5**, 371 (1960).
- ¹³J. M. Ziman, *Principles of the Theory of Solids* (Cambridge University Press, London, 1972).
- ¹⁴I. S. Gradshteyn and I. M. Ryzhik, *Table of Integrals, Series and Products* (Academic, San Diego, 1980).
- ¹⁵N. F. Mott and H. Jones, *The Theory of the Properties of Metals and Alloys* (Oxford University Press, New York, 1936).
- ¹⁶Z. W. Lu, S. H. Wei, and A. Zunger, Phys. Rev. B **44**, 10 470 (1991).
- ¹⁷Our KKR-CPA calculations were done adding a little (10^{-3} Ry) imaginary part to the energies. This is equivalent to introducing finite lifetimes, much larger than those introduced by substitutional disorder and identical for all the electronic states.
- ¹⁸W. H. Butler and G. M. Stocks, Phys. Rev. B **29**, 4217 (1984).
- ¹⁹*Selected Values of the Thermodynamic Properties of Random Binary Alloys*, edited by R. Hultgren *et al.* (American Society for Metals, Metals Park, OH, 1973).